Tangled localization at the cortical division site of plant cells occurs by several mechanisms

Carolyn G. Rasmussen*, Brian Sun and Laurie G. Smith

University of California, San Diego, Section of Cell and Developmental Biology, 9500 Gilman Dr., La Jolla, CA 92093-0116, USA

*Author for correspondence (cgrasmussen@ucsd.edu)

Accepted 22 September 2010
Journal of Cell Science 124, 270-279

doi:10.1242/jcs.073676

Summary

TANGLED (TAN) is the founding member of a family of plant-specific proteins required for correct orientation of the division plane. *Arabidopsis thaliana* TAN is localized before prophase until the end of cytokinesis at the cortical division site (CDS), where it appears to help guide the cytokinetic apparatus towards the cortex. We show that TAN is actively recruited to the CDS by distinct mechanisms before and after preprophase band (PPB) disassembly. Colocalization with the PPB is mediated by one region of TAN, whereas another region mediates its recruitment to the CDS during cytokinesis. This second region binds directly to POK1, a kinesin that is required for TAN localization. Although this region of TAN is recruited to the CDS during cytokinesis without first colocalizing with the PPB, pharmacological evidence indicates that the PPB is nevertheless required for both early and late localization of TAN at the CDS. Finally, we show that phosphatase activity is required for maintenance of early but not late TAN localization at the CDS. We propose a new model in which TAN is actively recruited to the CDS by several mechanisms, indicating that the CDS is dynamically modified from prophase through to the completion of cytokinesis.

Key words: Arabidopsis, TANGLED, Cytokinesis, PPB, Phragmoplast, Phosphatase, Tobacco BY-2

Introduction

Several components of the cell division machinery are common to both plants and animals. One example is the spindle that separates the chromosomes during metaphase and anaphase. In animal cells, the orientation of the spindle determines the future division plane (Rappaport, 1986). By contrast, two unique (plant-specific) microtubule and microfilament structures are observed during somatic cell division in most land plants, reflecting their distinctive way of performing cytokinesis and orienting their cell division planes relative to other eukaryotes. The first is a pre-prophase band (PPB) that forms at the cell cortex before prophase and surrounds the premitotic nucleus (Mineyuki, 1999). The location of the PPB predicts the future division plane (Mineyuki, 1999), but the PPB is disassembled as the spindle forms. After the spindle has separated the chromosomes, the second plant-specific cytoskeletal structure, a cytokinetic apparatus known as the phragmoplast, is created. The phragmoplast functions as a scaffold to guide the formation of the new cell wall (Jurgens, 2005). It arises from the spindle remnants between the daughter nuclei and subsequently expands centrifugally to attach the new cell wall at the cortical division site (CDS) previously occupied by the PPB. A longstanding problem in the plant cytokinesis field has been to understand how the cell 'remembers' the location of the PPB during mitosis and cytokinesis (Lloyd and Buschmann, 2007).

There are several lines of evidence that suggest that the PPB helps determine the final position of new cell wall insertion. The PPB accurately predicts the division plane (Mineyuki, 1999; Van Damme et al., 2007; Muller et al., 2009). Moreover, dividing cells that fail to form a PPB have defects in division plane orientation. For example, *Adiantum capilus-veneris* cells lacking PPBs show late phragmoplast misorientation and oblique cell plate insertion (Mineyuki et al., 1991). In *Arabidopsis thaliana* (McClinton and Sung, 1997; Camilleri et al., 2002; Kawamura et al., 2006; Azimzadeh et al., 2008) and *Zea mays* (Wright et al., 2009), mutants that fail to make PPBs display cells with random planes of division. Cultured *A. thaliana* (Chan et al., 2005) and tobacco cells (Vanstraelen et al., 2006) lacking PPBs also exhibit random division planes. Together, these experiments highlight the importance of the PPB in establishing the division plane.

Following PPB disassembly, the CDS is marked throughout the remainder of the cell cycle by local depletion of cortical F-actin and the kinesin KCA1 (Cleary et al., 1992; Liu and Palevitz, 1992; Sano et al., 2005; Vanstraelen et al., 2006). The significance of these negative CDS markers is not completely clear, but their formation depends on microtubules, suggesting that the PPB is required to create these marks (Palevitz, 1987; Cleary et al., 1992; Liu and Palevitz, 1992; Sano et al., 2005; Vanstraelen et al., 2006). In another experiment, PPBs were depolymerized with a reversible microtubule-destabilizing drug, then washed out to allow spindle formation and the completion of mitosis. In most cases, the phragmoplasts correctly oriented their expansion towards the CDS (Marcus et al., 2005). One way that PPB microtubules might locally modify the composition of the plasma membrane and cell cortex is through local stimulation of endocytosis, which occurs at a higher frequency in the PPB zone (Dhonukshe et al., 2005; Karahara et al., 2009; Karahara et al., 2010), possibly leading to localized depletion of KCA1 and actin nucleation or stabilization factors. Although the role of the PPB in division plane establishment remains to be fully elucidated, the prevailing view holds that the PPB initially 'sets up' the CDS, which is then statically maintained after PPB disassembly throughout mitosis and cytokinesis.

A. thaliana TANGLED (TAN), a homolog of a newly described highly basic protein in maize with microtubule binding activity (Smith et al., 2001), was the first protein identified that positively marks the CDS throughout mitosis and cytokinesis (Walker et al., 2007). TAN–YFP forms a broad ring that colocalizes with the PPB and remains at the CDS after PPB disassembly. After mitosis, the TAN ring sharpens into a tightly focused, punctate ring as the

phragmoplast expands towards the CDS (Walker et al., 2007). As demonstrated earlier for maize TAN (Cleary and Smith, 1998), *A. thaliana* TAN is not required for PPB formation or positioning, but facilitates the guidance of expanding phragmoplasts to the CDS (Walker et al., 2007). Together, these observations led to the hypothesis that TAN functions as a cortical marker that 'remembers' the location of the PPB via its retention at the CDS during mitosis and cytokinesis. Contrary to this view, we show that distinct regions of TAN mediate its localization to the CDS at different stages of cell division. Our findings imply that TAN is not statically retained at the CDS following PPB disassembly (e.g. via a tethering mechanism), but rather actively recruited there by distinct mechanisms before and after PPB disassembly.

Results

Two distinct regions of TANGLED are required for early and late TAN localization at the cortical division site

Full length *A. thaliana* TAN–YFP localizes to the cortical division site (CDS) throughout mitosis and cytokinesis, yet has no recognizable domains (Walker et al., 2007). We created a set of deletion constructs to identify the domains required for the CDS localization of TAN. The TAN ORF was divided into five roughly equal pieces, subsequently referred to as Regions I–V, and deletion constructs were created which removed one or more regions with the remaining coding sequence fused to the yellow fluorescent protein (YFP) gene. These TAN deletion–YFP fusion constructs were then transformed into *A. thaliana* containing the live cell microtubule marker Cerulean fluorescent protein (CFP) fused to α-tubulin (CFP–TUA) (Kirik et al., 2007), which allowed identification of mitotic and cytokinetic structures. We previously demonstrated that full-length TAN–YFP expressed from either the CaMV 35S promoter or the *TAN* native promoter localized similarly to the CDS in dividing root tip cells of transgenic *A. thaliana* (Walker et al., 2007). In the current study, all TAN–YFP constructs were expressed from the 35S promoter and at least five independent transgenic lines were observed for each construct. TAN localization was assessed in dividing cells at the root tip. Stages of division were identified by three microtubule structures: the preprophase band (PPB), the spindle and the phragmoplast.

Full length TAN–YFP localized to the CDS during all stages of mitosis and cytokinesis as described previously (Walker et al., 2007) (Fig. 1A, Table 1). TAN–YFP formed a broad ring that colocalized with the PPB, and narrowed during cytokinesis as the phragmoplast expanded. In addition to CDS localization, we often observed nuclear or nucleolar localization of TAN–YFP. For example, in cells where full-length TAN–YFP colocalized with the PPB, 41% (n=17) of cells also had nuclear or nucleolar localization. Nuclear or nucleolar location was also often observed for TAN deletion–YFP constructs. We cannot currently address the significance of this localization but we note that some proteins containing basic stretches, such as those found in TAN, passively diffuse into and are preferentially retained in the nucleolus (van Eenennaam et al., 2001; Meng et al., 2007). We took advantage of nuclear, nucleolar and/or cytoplasmic localization along with CDS localization to identify plants and cells in which TAN–YFP deletion derivatives were expressed. All results presented below are for cells in which YFP fluorescence was observed somewhere in the cell, demonstrating that the fusion protein was present whether or not it localized to the CDS.

First, we determined the localization of TAN missing Region I (TAN-IΔ–YFP). TAN-IΔ–YFP colocalized with the PPB, but was rarely observed at the CDS in cells with spindles and never during phragmoplast expansion (Fig. 1B, Table 1). We determined the timing of disappearance of TAN-IΔ–YFP from the CDS by observing four cells expressing this construct as they progressed through the cell cycle. In the 6 minute time course shown in Fig. 2A, TAN-IΔ–YFP was initially present at the CDS in a cell undergoing the transition from PPB to spindle, but disappeared after PPB microtubules fully disassembled (arrow, Fig. 2A). A neighboring cell in preprophase or prophase maintained TAN-IΔ–YFP signal at the CDS throughout this time course (Fig. 2A, arrowhead) showing that the disappearance of YFP signal at the CDS in the other cell is not due to photobleaching. In the other

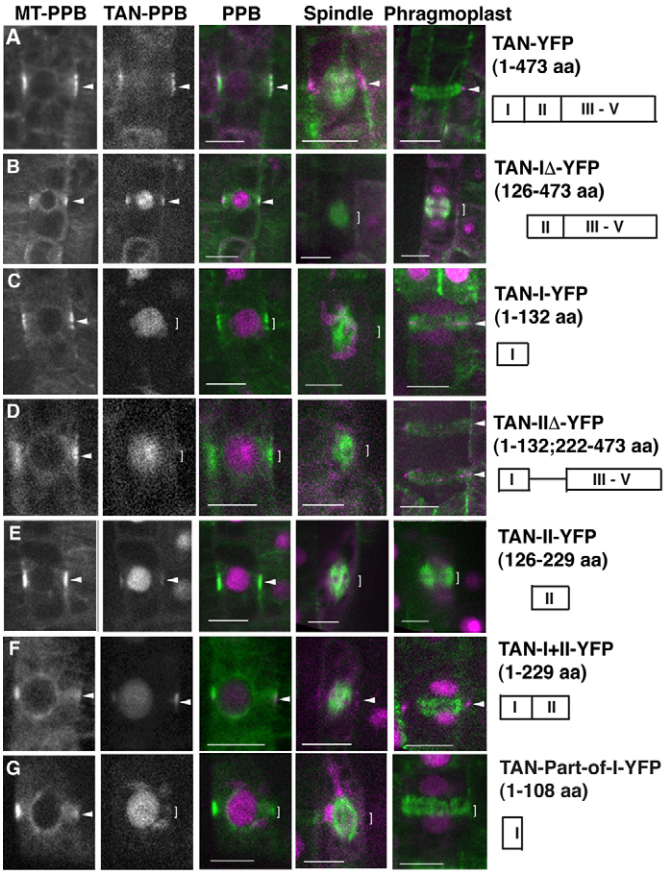

Fig. 1. Localization of TAN–YFP deletion constructs in CFP–TUA-labeled *A. thaliana* roots. (**A–G**) PPB microtubules labeled with CFP–TUA are shown in the first column, with the corresponding TAN–YFP signals in the second column. Merged CFP–TUA (green) and TAN–YFP (magenta) images of PPBs are shown in the third column. CFP–TUA (green) and TAN–YFP (magenta) merged images are shown of representative cells containing spindles (fourth column) and phragmoplasts (fifth column). Overlap between magenta and green signals appears white. Arrowheads indicate the cortical division site (CDS) in cells containing a TAN–YFP or CFP–TUA ring. Brackets indicate the location of the CDS in cells where the TAN–YFP deletion construct does not form a ring. All images are single optical planes except the phragmoplasts in A,C,D and the spindle and phragmoplast in E,F,G, which are three-dimensional reconstructions. For the PPB in F, an optical slice of a 3D reconstruction was used to more clearly show the TAN–YFP ring. In the midplane views shown here, cortical rings appear as an opposing pair of vertical lines (broad rings) or dots (sharp rings). Each deletion construct label contains the amino acids included in parentheses with a schematic diagram illustrating the portion of the protein included in the construct below. Scale bar: 10 μm.

Table 1. Quantitative analysis of TAN–YFP rings and microtubule structures labeled with CFP–TUA in living *A. thaliana* root cells

Construct (amino acids)	PPB	Spindle	Phragmoplast
TAN–YFP (1–473)	+ (100%, *n*=26)	+ (100% *n*=9)	+ (100%, *n*=37)
TAN-IΔ–YFP (126–473)	+ (100%, *n*=62)	–/+ (25%, *n*=12)	– (0%, *n*=42)
TAN-I–YFP (1–132)	– (0%, *n*=31)	– (0%, *n*=10)	+ (92%, *n*=24)
TAN-IIΔ–YFP (1–132; 222–473)	– (0%, *n*=31)	– (0%, *n*=15)	+ (100%, *n*=27)
TAN-II–YFP (126–229)	+ (90%, *n*=39)	– (0%, *n*=10)	– (0%, *n*=16)
TAN-I+II–YFP (1–229)	+ (98%, *n*=49)	+/– (50%, *n*=12)	+ (95%, *n*=42)
TAN-Part-of-I–YFP (1–108)	– (0%, *n*=28)	– (0%, *n*=7)	– (0%, *n*=14)
TAN-IIIΔ–YFP (1–195; 307–473)	+/– (62%, *n*=29)	+ (100%, *n*=12)	+ (100%, *n*=33)
TAN-IVΔ–YFP (1–290; 420–473)	+ (100%, *n*=21)	+ (100%, *n*=6)	+ (100%, *n*=32)
TAN-VΔ–YFP (1–420)	+ (100%, *n*=21)	+ (100%, *n*=9)	+ (100%, *n*=27)
TAN-III-V–YFP (222–473)	–/+ (6%, *n*=32)	–/+ (18%, *n*=11)	– (0%, *n*=22)

At least five independent transformants and/or their progeny were scored for each construct. Only observations with clear TAN–YFP deletion and CFP–TUA signal in the same cell were included in this analysis. *n* is the number of PPBs, spindles or phragmoplasts. +, almost all PPBs, spindles or phragmoplasts have TAN–YFP at the CDS; +/–, the majority of PPBs, spindles or phragmoplasts have TAN–YFP at the CDS; –/+, a minority of PPBs, spindles or phragmoplasts have TAN–YFP at the CDS; –, no PPBs, spindles or phragmoplasts have TAN–YFP at the CDS. The proportion of PPBs, spindles or phragmoplasts with TAN–YFP at the CDS is also given as a percentage.

three cells examined, TAN-IΔ–YFP was also maintained briefly at the CDS after PPB breakdown, but disappeared before the phragmoplast formed. These observations show that TAN Region I is not required for colocalization of TAN with PPBs, but is required for maintenance of TAN at the CDS after PPB disassembly.

We analyzed the localization of a TAN deletion containing only Region I (TAN-I–YFP) to determine whether this region is sufficient for localization of TAN at the CDS after PPB disassembly. Indeed, TAN-I–YFP localized to the CDS during phragmoplast expansion, but was absent from the CDS in cells with PPBs and spindles (Fig. 1C, Table 1). We assessed the timing of TAN-I–YFP appearance in five cells as they progressed through the cell cycle. During the 42 minute time course shown in Fig. 2B, a cell progressed from metaphase (with a spindle and no TAN-I–YFP ring) to telophase, when TAN-I–YFP appeared at the CDS as the phragmoplast expanded. Similarly, TAN-I–YFP appeared at the CDS as the phragmoplast expanded in the four other cells observed by time-lapse microscopy. Together, these data show that TAN Region I is necessary and sufficient for CDS localization during phragmoplast expansion but is not required for colocalization with PPBs.

TAN missing Region II (TAN-IIΔ–YFP), similarly to TAN-I–YFP, localized to the CDS during phragmoplast expansion (Fig. 1D, Table 1) but not in cells with PPBs or spindles. Similarly to TAN-IΔ–YFP, TAN Region II only (TAN-II–YFP) colocalized with PPBs, but was not observed at the CDS in cells with spindles or phragmoplasts (Fig. 1E, Table 1). These data show that Region II is not necessary for CDS localization during cytokinesis, but is necessary and sufficient to localize TAN to the CDS during preprophase and prophase.

Because TAN Regions I and II seemed to mediate most aspects of TAN–YFP localization at the CDS, we next assessed a TAN deletion containing only Regions I and II (TAN-I+II–YFP). Consistent with analysis of the localization of TAN Region I and Region II separately, showed that TAN-I+II–YFP colocalized with the PPB and localized to the CDS during phragmoplast expansion, demonstrating that these regions are sufficient for TAN–YFP localization to the CDS during preprophase or prophase and cytokinesis (Fig. 1F, Table 1). TAN-I+II–YFP was also localized as a faint CDS ring in 50% of cells with spindles. This could be because TAN-I+II–YFP is always localized at the CDS at the spindle stage but falls below the detection threshold half the time, or because other regions of TAN assist with its localization to the CDS at this stage. To address the second possibility, we observed TAN–YFP fusion constructs in which other regions (III, IV and V) were individually deleted. All three constructs localized to the CDS normally in cells with PPBs, spindles and phragmoplasts (Table 1). These data indicate that, individually, Regions III–V are not required for CDS localization at the spindle stage or any other stage of cell division. Finally, when TAN Region III–V was fused to YFP, it showed mostly cytoplasmic and/or nucleolar localization. Very occasionally, TAN-III–V–YFP colocalized with the PPB. TAN-III–V was also occasionally observed at the CDS during the spindle stage, but never during phragmoplast expansion (Table 1). From these data, we conclude that Regions III–V together make minor contributions to PPB and spindle stage TAN localization, optimizing TAN localization to the CDS at the spindle stage when combined with Regions I and II.

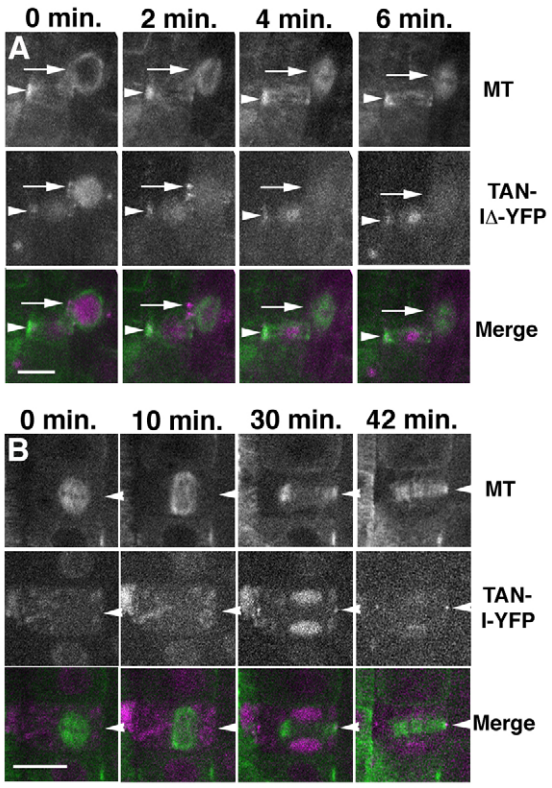

Fig. 2. Time courses illustrating the disappearance of TAN-IΔ–YFP and appearance of TAN-I–YFP during the cell cycle in *A. thaliana* root cells. Labels across the top indicate minutes elapsed, labels on the sides identify the images showing microtubules (MT, CFP–TUA), TAN–YFP deletion constructs, and TAN–YFP deletion constructs (magenta) and merged images (green). Areas of magenta and green overlap appear white. (**A**) CDS in a cell that is initially undergoing the PPB-to-spindle transition (arrows). The TAN-IΔYFP ring disappears as the cell advances to metaphase. In the cell below, arrowheads indicate the CDS in a preprophase or prophase cell with a MT PPB and TAN-IΔ–YFP ring that both persist throughout the time course (although only one side of the TAN-IΔ–YFP ring is clear in this 3D reconstruction). These images are 3D reconstructions of six 1 µm Z-slices. (**B**) CDS in a cell that initially in metaphase (containing a spindle), where a sharp TAN-I–YFP ring appears early in cytokinesis when the phragmoplast has formed and persists as the phragmoplast expands (arrowheads). These images are single focal planes. Scale bars: 10 µm.

POK1 interacts with Region I of TAN in the yeast two-hybrid system

Results for localization of TAN–YFP deletion derivatives suggested that TAN localization to the CDS is mediated by more than one mechanism: a Region-II-dependent mechanism that recruits TAN to the CDS initially, and a Region-I-dependent mechanism that recruits TAN to the CDS during cytokinesis. Previous data showed that a C-terminal fragment of a putative kinesin POK1 (Muller et al., 2006), and full-length POK1 (Xu et al., 2008), binds to TAN in a yeast two-hybrid assay and in planta (Xu et al., 2008). In addition, studies on TAN–YFP localization in mutants lacking both POK1 and a closely related kinesin, POK2, showed that these kinesins are essential for TAN localization at the CDS during phragmoplast expansion. POK1 and POK2 also promote TAN colocalization with PPBs, although they are not strictly required for it (Walker et al., 2007). These data led us to hypothesize that POKs function by separate mechanisms to promote TAN localization at early versus late stages of cell division. To investigate this hypothesis, we tested all of the TAN deletion constructs for their ability to bind to POK1 in a directed yeast two-hybrid assay. All deletion derivatives that lacked Region I failed to bind to POK1, whereas all those containing Region I bound to POK1, including Region I alone (Table 2, supplementary material Fig. S1). Thus, Region I is necessary and sufficient for interaction of TAN with POK1 in yeast, as it is for localization of TAN to the CDS during cytokinesis. This suggests that POK1 localizes TAN to the CDS during cytokinesis via direct binding, and functions by a different, indirect mechanism to promote TAN colocalization with PPBs. Interestingly, a smaller section of Region I (residues 1–108, the N-terminal 80%) interacted efficiently with POK1 in yeast (Table 2; supplementary material Fig. S1), but was not sufficient for localization to the CDS in planta (Table 1; Fig. 1G). This finding suggests that POK1 binding is necessary but not sufficient for TAN localization to the CDS during cytokinesis.

PPBs are required for localization of TAN at the CDS during mitosis and cytokinesis

Initial recruitment of TAN to the CDS (i.e. colocalization with the PPB) requires intact microtubules (Walker et al., 2007). However, once formed, broad TAN rings were maintained at the CDS when microtubules were depolymerized with oryzalin, indicating that TAN maintenance at the CDS during prophase does not require intact microtubules (Walker et al., 2007). The remarkable ability of TAN-I–YFP to localize to the CDS during cytokinesis without previous association with the PPB raises the question of whether the PPB is necessary for TAN localization at the CDS during cytokinesis. Because TAN is implicated in guidance of expanding phragmoplasts to the CDS (Cleary and Smith, 1998; Walker et al., 2007) this question fundamentally challenges the role of the PPB in division plane maintenance in plant cells. This question could not be addressed in our previous drug treatment experiments because cells do not proceed through mitosis and cytokinesis in oryzalin (because microtubules are required for both processes). Previously, we showed that TAN fails to localize to the CDS at all

Table 2. POK-1 and TAN interaction in yeast two-hybrid system and corresponding summary of localization in planta

Construct	POK-1 binding	TAN–YFP deletion colocalized with PPB	TAN–YFP deletion at the CDS during cytokinesis
TAN (1–473) [I][II][III–V]	+	+	+
TAN-IΔ (126–473) [II][III–V]	–	+	–
TAN-I (1–132) [I]	+	–	+
TAN-IIΔ (1–132; 222–473) [I]——[III–V]	+	–	+
TAN-II (126–229) [II]	–	+	–
TAN-I+II (1–229) [I][II]	+	+	+
TAN-Part-of-I (1–108) [ ]	+	–	–

stages of division in *fass* mutants in which PPBs do not form (Walker et al., 2007). However, we cannot conclude from that observation that PPBs are required for TAN localization during mitosis and cytokinesis because FASS, the B″ regulatory subunit of the PP2A phosphatase, might have other roles in promoting TAN localization to the CDS besides promoting PPB formation (see next section).

We used bright-yellow-2 (BY-2) tobacco cells to test whether the PPB is required for TAN localization at the CDS during mitosis and cytokinesis. BY-2 cells are uniquely well suited for experiments requiring both a high mitotic index and PPBs (Nagata and Kumagai, 1999). In addition, BY-2 cells contain at least one TAN homolog based on available EST sequence (http://mrg.psc.riken.go.jp/strc/index.htm), suggesting that TAN function is conserved. *A. thaliana* TAN–YFP expressed from the CaMV 35S promoter was transformed into BY-2 cells to establish AYS9, which divided with similar kinetics compared with an untransformed cell line. TAN–YFP localization in BY-2 cells was equivalent to that seen in *A. thaliana*, as determined using a BY-2 line coexpressing CFP–TUA and *A. thaliana* TAN–YFP, AYS9CT5. Specifically, broad TAN rings were observed in cells with PPBs (n=74) or spindles (n=18) and sharp TAN rings were observed in cells with phragmoplasts (n=42) (Fig. 3). Similarly to TAN–YFP in *A. thaliana*, the TAN–YFP ring sharpened in BY-2 cells as the phragmoplast expanded, and disappeared shortly after phragmoplast disassembly (supplementary material Fig. S2).

To achieve a high mitotic index, block PPB formation, and then allow cells to proceed through mitosis and cytokinesis, we used a two-step synchronization method (Kumagai-Sano et al., 2006). The experimental design is outlined schematically in Fig. 4A. AYS9 cells expressing TAN–YFP were first treated with aphidicolin (a DNA synthesis inhibitor that blocks cells in early S phase), then

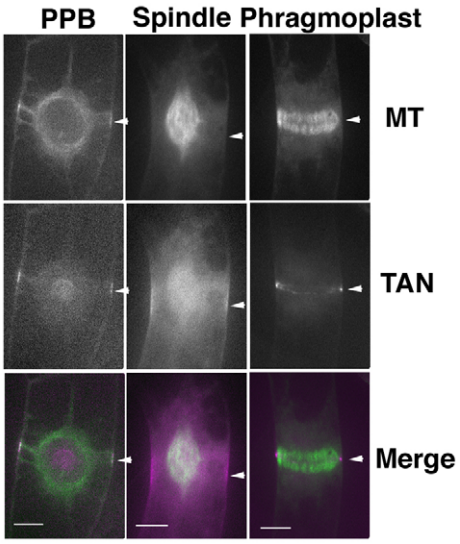

Fig. 3. Localization of *A. thaliana* full-length TAN–YFP in transgenic tobacco BY-2 cells. 35S-driven TAN–YFP (TAN) localization with coexpressed CFP–TUA (MT) during preprophase or prophase (PPB), metaphase (spindle) and cytokinesis (phragmoplast). In the merged images, MTs are false colored green and TAN is false colored magenta. Overlapping signal is white. As described in the text for transgenic *A. thaliana* root cells, and visible in the BY-2 cell with a PPB, TAN–YFP is often (59% of 122 PPB-containing cells examined) localized to nuclei or nucleoli in BY-2 cells as well as to the CDS. Scale bar: 15 μm.

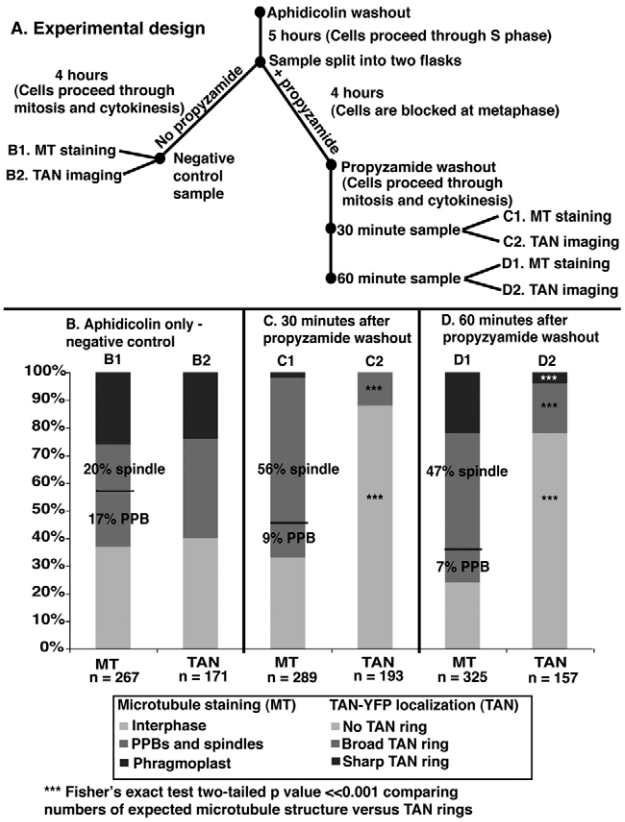

Fig. 4. Evidence that PPBs are required for TAN–YFP localization during mitosis and cytokinesis. (**A**) Schematic diagram outlining experiment. (**B–D**) Quantitative analysis of microtubule structures determined by fixation and immunofluorescent labeling (B1,C1,D1) and of TAN–YFP rings by live cell microscopy (B2,C2,D2). Results are shown for a single experiment representative of three experiments of this type conducted. ***P<<0.001, Fisher's exact test; highly significant differences were found between the proportion of cells having or lacking a TAN–YFP ring compared with the type of microtubule array expected if the cells had not been treated with propyzamide.

washed and later treated with the microtubule-depolymerizing drug propyzamide. Propyzamide allows cells to progress through prophase (without PPBs) but blocks progression into metaphase, causing cells to accumulate at the prophase–metaphase transition. Upon washout of propyzamide, most cells are expected to proceed through metaphase and cytokinesis without first forming a PPB. AYS9 cells treated with aphidicolin and subsequently with (or without) propyzamide were sampled at various times during the procedure. Each sample was split into two aliquots: one that was observed directly for TAN–YFP rings in live cells, and one that was fixed and stained for microtubules.

Cells that had been synchronized with aphidicolin but not treated with propyzamide were examined to confirm that the proportion of cells with specific microtubule structures in fixed cells was correlated with the proportion of cells having the expected type of TAN ring in live cells. As shown in Fig. 4B, the proportion of cells that have broad TAN rings (36%) was correlated with the proportion of cells containing PPBs and spindles (37%), and the proportion of cells that had a sharp TAN ring (24%) was correlated with the proportion of cells containing phragmoplasts (26%). Moreover, the

proportion of cells lacking a TAN ring (40%) was correlated with the proportion having an interphase microtubule array (37%). The proportion of cells containing each type of microtubule array was statistically indistinguishable [$P>0.1$ using Fisher's exact test (FET)] from the proportion having the expected TAN–YFP localization pattern. As expected, when cells treated with propyzamide were washed to allow mitosis to proceed for 30 minutes, they had a high proportion of spindles (56%) and fewer PPBs (9%). If propzyamide treatment did not affect TAN–YFP localization at the spindle stage, the expected percentage of broad rings would be equivalent to the proportion of cells with spindles and PPBs (65%). By contrast, we observed that only 12% of cells had broad TAN–YFP rings, similarly to the proportion containing a PPB (9%) (Fig. 4, compare C1 with C2; $P>0.1$, FET). At 60 minutes after propyzamide washout, 47% of cells contained spindles, whereas 7% had PPBs for a total of 54% of cells expected to contain broad TAN–YFP rings if propyzamide had no effect. However, only 18% of cells had broad TAN–YFP rings at 60 minutes. Thus, at both time points, the proportion of cells having broad TAN–YFP rings was significantly lower than expected if propyzamide had no effect on TAN localization at the spindle stage ($P<<0.01$, FET). From these data, we infer that cells which produced a PPB also localized TAN normally as a broad ring, but those that made a spindle without first forming a PPB did not form TAN broad rings. Sixty minutes after propyzamide washout, 22% of cells had phragmoplasts but only 4% had sharp TAN–YFP rings (Fig. 4B, compare D1 and D2 with B1 and B2; $P<<0.01$, FET). These observations suggest that cells which proceeded through metaphase and cytokinesis after propyzamide washout without first forming a PPB did not form sharp TAN–YFP rings. These data support the conclusion that the presence of a PPB during prophase is necessary for correct localization of TAN to the CDS during mitosis and cytokinesis.

To confirm these findings, additional experiments were carried out using AYS9CT5 cells, which are a BY-2 line coexpressing TAN–YFP and CFP–TUA. AYS9CT5 cells were synchronized using the two-step synchronization protocol outlined in Fig. 4A. Sixty minutes after propyzamide washout, 100% of cells with a PPB also had a broad TAN–YFP ring ($n=11$), whereas only 6% of cells with a spindle also had a broad TAN–YFP ring ($n=2/18$; these two could have made a PPB before forming a spindle). Representative cells are shown in Fig. 5A. In time course experiments, a cell with a PPB and a broad TAN–YFP ring shortly after propyzamide treatment and washout showed TAN–YFP localization at the CDS throughout mitosis and cytokinesis (Fig. 5B). By contrast, a cell from an equivalent sample that initially had a spindle and lacked a broad TAN–YFP ring failed to form a TAN–YFP ring as it proceeded through mitosis and cytokinesis (Fig. 5C). These observations further support the conclusion that the presence of a PPB during prophase is necessary for TAN–YFP localization to the CDS during mitosis and cytokinesis.

Inhibition of PP2A activity causes loss of broad TAN rings, but does not alter sharp TAN ring localization

Previous observations demonstrated that TAN localization to the CDS requires the *FASS* gene product (Walker et al., 2007), also called TONNEAU2, a B″ regulatory subunit of a PP2A phosphatase complex (Camilleri et al., 2002). *fass* mutants have drastically misoriented cell division planes (Torres-Ruiz and Jurgens, 1994). These cells fail to form PPBs yet are still capable of producing a spindle and phragmoplast (McClinton and Sung, 1997). When

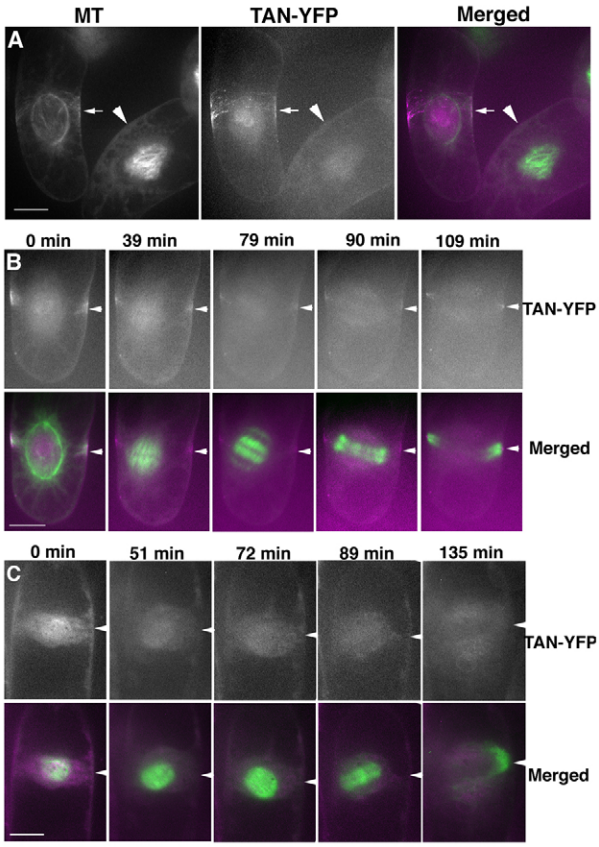

Fig. 5. TAN–YFP and CFP–TUA localization in BY-2 cells synchronized by the two-step method. The majority of cells (>50%) form a spindle within 60 minutes after propyzamide wash out and mitosis proceeds, whereas a minority of cells (~10%) form PPBs before proceeding through mitosis. TAN–YFP is false colored magenta and CFP–TUA is false colored green. (**A**) The cell on the left formed a PPB (arrow), whereas the cell on the right formed a spindle (an arrowhead indicates the predicted CDS for this cell). TAN–YFP colocalizes with the PPB (arrow) but is not observed at the CDS in the cell with a spindle. (**B**) Time course following a cell with a PPB and a corresponding TAN–YFP ring (arrowhead), which persisted as the cell completed mitosis and cytokinesis. (**C**) Time course following a cell with a spindle and lacking a TAN–YFP ring. TAN–YFP was not observed at the CDS (arrowhead) from the spindle stage through phragmoplast expansion. This phragmoplast rotated during expansion to create an askew division plane. Scale bars: 20 μm.

TAN–YFP localization was assessed in mitotic and cytokinetic cells of *fass* mutant roots, TAN was never observed at the CDS (Walker et al., 2007). We sought to clarify whether phosphatase activity is required for TAN localization or whether lack of TAN localization in *fass* mutants is merely due to a lack of PPBs. To address this question, we treated tobacco BY-2 cells expressing *A. thaliana* TAN–YFP (AYS9 cells) with the irreversible PP2A and PP1 phosphatase inhibitor okadaic acid (OA). Unlike the situation in *fass* mutants, where all cells proceed through division without a PPB, this approach allowed us to inhibit phosphatase activity in cells undergoing mitosis and cytokinesis that previously did have a PPB.

AYS9 cells were synchronized using aphidicolin, and sampled at 6, 7 and 8 hours after aphidicolin washout to determine the proportion having broad or sharp TAN–YFP rings (Fig. 6). OA (1

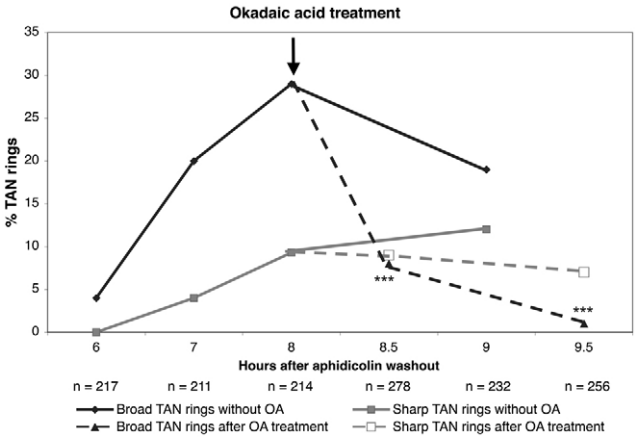

Fig. 6. Effects of inhibition phosphatase activity by okadaic acid on maintenance of TAN–YFP rings in dividing BY-2 cells. Time course following aphidicolin (S phase) cell synchronization (time sequence refers to time after aphidicolin washout). Before the 8 hour time point, the number of broad and sharp TAN rings gradually increased, indicating a significant proportion of cells entering mitosis and cytokinesis, as expected for synchronized cells. 1 μM OA was added 8 hours after aphidicolin washout (arrow) and TAN–YFP rings were counted 30 and 90 minutes later (8.5 and 9.5 hour time points, dashed lines). The control population is also plotted here to show the number of broad and sharp TAN–YFP rings observed in the absence of OA at 9 hours after aphidicolin washout (solid lines). More than 200 cells were examined for TAN–YFP rings at each time point. This experiment was conducted twice with similar results. Results from one experiment are shown. ***P<<0.001, Fisher's exact test. A highly significant difference was found between TAN–YFP rings counted before and after OA treatment for each time point.

μM) was added at 8 hours and cells were sampled again 30 and 90 minutes later (8.5 hour and 9.5 hour time points in Fig. 6). As shown in Fig. 6, the proportion of cells with broad TAN–YFP rings (found in cells with PPBs or spindles) declined sharply after addition of OA from 29% before treatment to 8% after 30 minutes and 1% after 90 minutes (P<<0.001, FET). By contrast, the proportion of cells with sharp TAN–YFP rings (found in cells undergoing cytokinesis) did not significantly change during the 90 minutes of OA treatment (Fig. 6; 9.3% before treatment, 9% after 30 minutes and 7% after 90 minutes with no significant difference observed between these populations by FET, P>0.1). Similar results from an independent experiment are shown in supplementary material Fig. S3. These data indicate that disruption of PP2A and/or PP1 phosphatase activity in cells that had already formed a sharp TAN–YFP ring did not alter that localization, but caused loss of broad TAN–YFP rings. OA has been shown to disrupt microtubule structures, thereby blocking progression of the cell cycle at multiple points (Hasezawa and Nagata, 1992). However, loss of broad rings cannot be readily attributed to effects of OA on microtubules, because previous data showed that maintenance of broad TAN–YFP rings at the CDS was unaffected by depolymerization of microtubules with oryzalin (Walker et al., 2007). Thus, these results suggest that PP2A and/or PP1 function is required for TAN maintenance at the CDS in cells with PPBs and spindles, but not in cells undergoing cytokinesis.

Discussion

TANGLED (TAN) is required for proper orientation of division planes in plant cells. TAN acts to guide the expanding phragmoplasts to the cortical division site (CDS) (Cleary and Smith, 1998; Walker et al., 2007). CDS localization of TAN through the completion of cytokinesis is presumably important for orienting the division plane, but previous work on TAN yielded no mechanistic insights as to how TAN is maintained at the CDS after PPB disassembly. In this paper, we show that TAN is localized to the CDS by at least two distinct mechanisms involving different regions of TAN and different interactions with other cellular components (microtubules, POK kinesins and phosphatase activity). A model is presented in Fig. 7, which summarizes our new findings within the temporal framework of the cell cycle.

As shown in Fig. 7, TAN is recruited to the CDS initially as the PPB forms. This initial recruitment requires microtubules as well as FASS (Walker et al., 2007), a PP2A phosphatase B″ regulatory subunit (Camilleri et al., 2002), which is also required for PPB formation (McClinton and Sung, 1997). In this study, we show that the initial recruitment and early maintenance of TAN at the CDS is mediated by Region II of TAN. Region II is both necessary and sufficient for TAN colocalization with PPBs throughout the completion of prophase. Okadaic acid experiments presented here provide evidence that maintenance of broad TAN rings also depends on PP2A and/or PP1 phosphatase activity. Thus, PP2A and/or PP1 phosphatase appears to promote TAN localization at the CDS in two ways: first by promoting formation of the PPB, and later by a microtubule-independent mechanism, where it acts to maintain TAN–YFP at the CDS through metaphase. The *Zea mays FASS* homologs *dcd1* and *add1*, similarly to *FASS*, are required for PPB formation. Intriguingly, DCD1 and ADD1 colocalize with the PPB and remain at the CDS throughout metaphase (Wright et al., 2009). It is tempting to speculate that TAN is a direct target of a FASS–DCD1–ADD1-containing PP2A complex, and that its dephosphorylation by this complex stabilizes it at the CDS through metaphase. A large-scale phosphoproteomic study using *A. thaliana* cultured cells (Sugiyama et al., 2008) has identified several phosphorylation sites in TAN, and many more potential phosphorylation sites are present. Perhaps phosphorylation of TAN might mediate its interaction with PPB microtubules, whereas subsequent dephosphorylation might permit microtubule-independent maintenance at the CDS. Phosphoregulation of microtubule binding affinity might explain why TAN, which has in vitro microtubule binding activity (Smith et al., 2001), only colocalizes in vivo with PPB microtubules and does not appear to associate with other microtubule structures.

Requirements for TAN localization during mitosis are more complex than those for localization during preprophase or prophase and cytokinesis (Fig. 7). Drug treatments causing cells to enter mitosis without forming PPBs provided evidence that TAN–YFP localization in cells with spindles depends on the previous presence of a PPB. Regions I and II are both required for CDS location in cells with spindles: neither Region I nor Region II alone were sufficient for CDS localization at this stage, but in combination they directed formation of faint TAN rings in half the spindle-stage cells observed. Regions III–V of TAN appear to assist its CDS localization at this stage because full-length TAN–YFP was always observed at the CDS during mitosis. However, Regions III–V alone are rarely sufficient for TAN–YFP localization at the CDS in cells with spindles, and none of these regions is required individually at this stage. Thus, a combination of mechanisms might operate to maintain TAN at the CDS during mitosis.

Later in the cell cycle, TAN localization to the CDS is controlled by Region I of TAN, which is both necessary and sufficient for

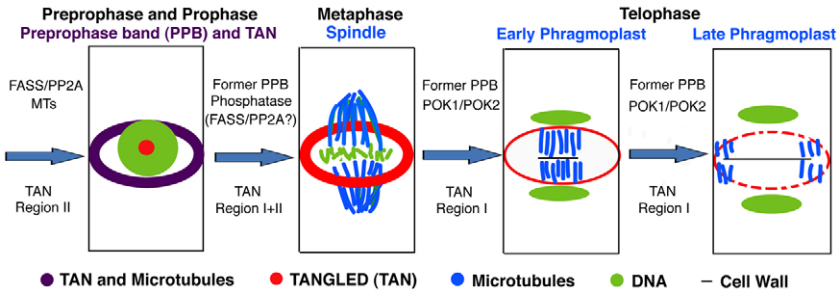

Fig. 7. Model summarizing the requirements for TAN–YFP localization at the CDS at different stages of the cell cycle, highlighting the dynamic nature of CDS maintenance after PPB disassembly. The blue arrows indicate transitions between the illustrated stages. Shown above these arrows are factors required for TAN localization to the CDS during the subsequent stage. Regions of TAN that are required for different temporal localization to the CDS are indicated below the arrows.

TAN localization as a sharp ring during phragmoplast expansion (Fig. 7). In the yeast two-hybrid system, TAN Region I is also necessary and sufficient for interaction with the C-terminus of POK1, a kinesin that is involved in proper orientation of the division plane and in TAN–YFP localization to the CDS (Muller et al., 2006; Walker et al., 2007). Although POK1 and POK2 promote TAN colocalization with the PPB, they are not absolutely required for it, because *pok1;pok2* double mutants occasionally showed proper TAN–YFP colocalization with PPBs (Walker et al., 2007). By contrast, TAN–YFP rings were never observed at the CDS in cells with spindles or phragmoplasts (Walker et al., 2007). Thus, POK1 and POK2 might have an indirect role in TAN colocalization with the PPB. Together with the current results, these data support the proposal that during cytokinesis TAN is recruited to the CDS through direct interaction with POK1, whereas its colocalization with the PPB is mediated by POK1/2 indirectly. Intriguingly, another protein that is localized to the CDS throughout the cell cycle, RAN-GAP1, shows a similar dependence on POK1/2 for localization during cytokinesis (Xu et al., 2008). RAN-GAP1 interacts with POK1 both in the yeast two-hybrid system and in planta. In *pok1;pok2* double mutants, RAN-GAP1 fails to localize to the CDS during cytokinesis, but still colocalizes with the PPB (Xu et al., 2008). Thus, both RAN-GAP1 and TAN might be recruited to the CDS during cytokinesis via a direct interaction with POK1.

The involvement of a kinesin suggests participation of microtubules in TAN and RAN-GAP1 localization at the CDS during cytokinesis, but it is not obvious how this would occur. The cortex itself is devoid of microtubules during mitosis and cytokinesis. Imaging of microtubules labeled at their plus ends with fluorescently tagged EB1 revealed that microtubules radiate from the surfaces of daughter nuclei towards the cortex during cytokinesis but they are not focused at the CDS (Chan et al., 2005; Dhonukshe et al., 2005), so do not provide obvious directional tracks to guide POK-mediated delivery of TAN to the CDS during cytokinesis. Alternatively, it is possible that POK1 is initially localized to the CDS through an interaction with PPB microtubules and remains there throughout mitosis and cytokinesis, where it could then recruit both TAN and RAN-GAP1 to the CDS during cytokinesis.

Cells that did not form a PPB lacked TAN–YFP rings in cells undergoing mitosis and cytokinesis. When the PPB does not form in propyzamide treated cells, the positional cues established by the PPB are missing. Thus, although TAN Region I localizes to the CDS during cytokinesis without previously colocalizing with PPBs, the PPB is still required for late TAN–YFP localization (Fig. 7). Together, these observations suggest that a PPB-dependent positional cue other than TAN itself marks the CDS after PPB disassembly in a way that permits recruitment of TAN to this site during cytokinesis by a mechanism that is dependent on Region I and POK. It is possible that this cue could be the PP2A subunit FASS, whose maize homologs DCD1 and ADD1 persist briefly at the CDS after PPB disassembly (Wright et al., 2009). However, there is no evidence that FASS localization itself is PPB dependent. Another possibility is that the positional cue is POK1/2; localization of these kinesin-like proteins throughout the cell cycle and their potential dependence on PPB formation will allow this possibility to be addressed.

AIR9, an essential microtubule binding protein, shows intriguing parallels with TAN. Similarly to TAN, AIR9 has two separate domains that are responsible for its localization at the CDS during different stages of cell division (Buschmann et al., 2006). The first domain colocalizes with PPBs whereas the second localizes to the CDS and the cell plate during cell plate insertion (Buschmann et al., 2006). This later localization of AIR9 appears to require an unknown signal from the former PPB: cell plates that insert at a site previously occupied by a PPB show AIR9 accumulation, whereas those that insert at aberrant locations do not (Buschmann et al., 2006). Full-length AIR9 does not localize at the CDS during the spindle stage or during phragmoplast expansion, but only later, as the cell plate inserts into the mother cell wall (Buschmann et al., 2006). Nevertheless, TAN and AIR9 are similar insofar as they both have separate domains mediating early versus late localization of CDS and require the PPB for late CDS localization.

The experiments presented here investigated the requirements for TAN localization to the CDS. Our data have revealed that CDS maintenance after PPB disassembly is an unexpectedly dynamic process. The CDS is not ‘set up’ by the PPB and subsequently maintained in a static manner, but rather continuously modified during mitosis and cytokinesis by several mechanisms. We expect that identification of other proteins that interact with TAN differentially throughout the cell cycle can provide insights into mechanisms by which the CDS is established and maintained to properly orient the division planes of plant cells.

Materials and Methods

Microscopy and image processing

A. thaliana was grown on half-strength MS [Murashige and Skoog salts (Murashige and Skoog, 1962), MP Biomedical] plates solidified with 0.8% agar held vertically in constant light or standard long day conditions (16 hours light, 8 hours dark). Seedlings between 5 and 10 days old were mounted in water and their root tips were observed using a spinning-disk confocal microscope set-up as described (Paredez et al., 2006; Walker et al., 2007). Briefly, CFP–TUA signal was excited with a 440 nm laser line and viewed with a 480/40 nm bandpass emission filter. TAN–YFP and various TAN–YFP deletion signals were excited with a 514 nm laser line and viewed with a 570/65 nm emission filter. A Roper Cascade 512b EM CCD camera was used to capture images. The confocal system was controlled using MetaMorph software v7 (Universal Imaging Corporation, Downington, PA). Z-stacks were collected using 1 or 2 µm steps. 3D reconstructions were assembled using Metamorph or ImageJ (http://rsbweb.nih.gov/ij/download.html). Image processing and false coloring was done with ImageJ, Adobe Photoshop CS and/or Adobe Illustrator CS. Only linear adjustments were applied to pixel values.

Plasmid construction and *A. thaliana* and *S. cerevisiae* transformation

Primer sequences used in this study are presented in supplementary material Table S1. Overlap PCR (Sambrook and Russell, 2001) was used to construct TAN–YFP deletion constructs using the TAN–YFP binary vector described (Walker et al., 2007) as the template. This vector contains the *A. thaliana* TAN cDNA from the *Ler* ecotype driven by the 35S promoter. When necessary, pGEMT (Promega) was used for subcloning of PCR products. All deletion constructs were ligated into the pAS yeast two-hybrid vector (Fan et al., 1997) (provided by the ABRC) or the TAN–YFP binary vector (replacing full-length TAN with the deletion derivative) using *Eco*RI and *Bam*HI restriction enzymes. Final plasmids used for yeast or *A. thaliana* transformations were sequenced to confirm that they did not contain errors.

A. thaliana containing CFP–TUA (Kirik et al., 2007) (a kind gift from Viktor Kirik) was transformed with TAN–YFP deletion constructs using the floral dip method (Clough and Bent, 1998) and transformants were selected on half-strength MS plates solidified with 0.8% agar with 50 mg/l kanamycin. Transformants were screened for YFP expression by microscopy and positive transformants were transplanted into soil. At least five independent transformants were analyzed for each TAN deletion derivative and/or their progeny for data presented in Table 1.

Yeast two-hybrid analysis

S. cerevisiae were transformed according to published methods (Gietz and Schiestl, 2007) using the pAD-POK1 construct (Muller et al., 2006) with pBD-TAN (Walker et al., 2007) as a positive control for comparison with interaction between pAD-POK1 and various TAN deletion constructs. The TAN deletion constructs were cloned into the pAS vector (Fan et al., 1997), which contains the Gal4 binding domain similarly to pBD. Positive yeast two-hybrid interaction was determined by growth on plates lacking histidine according to the manufacturer's instructions (Stratagene). Yeast transformants were plated in parallel with the empty-vector negative control. After 3 days of growth, photographs were taken of the plates. The colors were inverted in Photoshop (Adobe version CS) for clarity (supplementary material Fig. S1).

Tobacco cell culture

Tobacco BY-2 cells were a kind gift from Takashi Hotta and Bo Liu (University of California Davis, Davis, CA). BY-2 cells were maintained according to the protocols outlined (Nagata and Kumagai, 1999; Kumagai-Sano et al., 2006) and synchronized as previously described (Planchais et al., 1997; Kumagai-Sano et al., 2006). BY-2 cells were transformed using *A. tumefaciens* (An, 1985) using the TAN–YFP plasmid described (Walker et al., 2007) to create the line AYS9 and also with the CFP–TUA plasmid (Kirik et al., 2007), a kind gift from Viktor Kirik (Illinois State University, Bloomington-Normal, IL), to create AYS9CT5. Transformed calli were selected on either 100 mg/l Kan or 20 mg/l hygromycin plates solidified with 3 g/l phytagel. Small calli were screened by microscopy for CFP and/or YFP expression (Van Damme et al., 2004) and calli with consistent expression were transferred to liquid culture. Experiments using OA were performed according to (Hasezawa and Nagata, 1992). Briefly, AYS9 cells were blocked in S-phase using 3 μg/l aphidicolin, then the cells were washed and proceeded through mitosis and cytokinesis. 1 μM OA was added to liquid cultures 8 hours after aphidicolin washout (when cells contained both broad and sharp TAN rings), and AYS9 cells were observed at 30 and 90 minutes after addition of OA. Microtubule immunofluorescence microscopy of BY-2 microtubules was performed as described (Sugimoto et al., 2000) except antibody incubation times were reduced to 90 minutes and fixation was performed between 30 minutes and 18 hours. For live-cell imaging of BY-2 cells expressing *A. thaliana* TAN–YFP, micrographs were taken of random fields of view were taken of AYS9 cells for <10 minutes. Analysis of TAN–YFP localization was performed later.

We thank Bo Liu and Takashi Hotta for BY-2 cells and Viktor Kirik for the CFP–TUA plasmid and *A. thaliana* seeds. We thank Daniel van Damme and Toshiyuki Nagata for their very helpful advice regarding BY-2 cell culture. We thank John Humphries, Amanda Wright, Sabine Muller, Michelle Facette, Taehoun Kim, Ray Shao and three anonymous reviewers for their helpful comments on this manuscript. Finally, we thank the ABRC for materials used in this study. This work was supported by Postdoctoral Fellowship Grant #PF-08-280-01 from the American Cancer Society to C.G.R., and USDA grant 2006-35304-17342 to L.G.S.

Supplementary material available online at
http://jcs.biologists.org/cgi/content/full/124/2/270/DC1

References

An, G. (1985). High Efficiency transformation of cultured tobacco cells. *Plant Physiol.* **79**, 568-570.

Azimzadeh, J., Nacry, P., Christodoulidou, A., Drevensek, S., Camilleri, C., Amiour, N., Parcy, F., Pastuglia, M. and Bouchez, D. (2008). Arabidopsis TONNEAU1 proteins are essential for preprophase band formation and interact with centrin. *Plant Cell* **20**, 2146-2159.

Buschmann, H., Chan, J., Sanchez-Pulido, L., Andrade-Navarro, M. A., Doonan, J. H. and Lloyd, C. W. (2006). Microtubule-associated AIR9 recognizes the cortical division site at preprophase and cell-plate insertion. *Curr. Biol.* **16**, 1938-1943.

Camilleri, C., Azimzadeh, J., Pastuglia, M., Bellini, C., Grandjean, O. and Bouchez, D. (2002). The *Arabidopsis TONNEAU2* gene encodes a putative novel protein phosphatase 2A regulatory subunit essential for the control of the cortical cytoskeleton. *Plant Cell* **14**, 833-845.

Chan, J., Calder, G., Fox, S. and Lloyd, C. (2005). Localization of the microtubule end binding protein EB1 reveals alternative pathways of spindle development in Arabidopsis suspension cells. *Plant Cell* **17**, 1737-1748.

Cleary, A. L. and Smith, L. G. (1998). The *Tangled1* gene is required for spatial control of cytoskeletal arrays associated with cell division during maize leaf development. *Plant Cell* **10**, 1875-1888.

Cleary, A. L., Gunning, B. E. S., Wasteneys, G. O. and Hepler, P. K. (1992). Microtubule and F-actin dynamics at the division site in living Tradescantia stamen hair cells. *J. Cell Sci.* **103**, 977-988.

Clough, S. J. and Bent, A. F. (1998). Floral dip: a simplified method for Agrobacterium-mediated transformation of Arabidopsis thaliana. *Plant J.* **16**, 735-743.

Dhonukshe, P., Mathur, J., Hulskamp, M. and Gadella, T. W., Jr (2005). Microtubule plus-ends reveal essential links between intracellular polarization and localized modulation of endocytosis during division-plane establishment in plant cells. *BMC Biol.* **3**, 11.

Fan, H. Y., Hu, Y., Tudor, M. and Ma, H. (1997). Specific interactions between the K domains of AG and AGLs, members of the MADS domain family of DNA binding proteins. *Plant J.* **12**, 999-1010.

Gietz, R. D. and Schiestl, R. H. (2007). Quick and easy yeast transformation using the LiAc/SS carrier DNA/PEG method. *Nat. Protoc.* **2**, 35-37.

Hasezawa, S. and Nagata, T. (1992). Okadaic acid as a probe to analyse the cell cycle progression in plant cells. *Bot. Acta* **105**, 63-69.

Jurgens, G. (2005). Cytokinesis in higher plants. *Annu. Rev. Plant Biol.* **56**, 281-299.

Karahara, I., Suda, J., Tahara, H., Yokota, E., Shimmen, T., Misaki, K., Yonemura, S., Staehelin, L. A. and Mineyuki, Y. (2009). The preprophase band is a localized center of clathrin-mediated endocytosis in late prophase cells of the onion cotyledon epidermis. *Plant J.* **57**, 819-831.

Karahara, I., Staehelin, L. A. and Mineyuki, Y. (2010). A role of endocytosis in plant cytokinesis. *Commun. Integr. Biol.* **3**, 36-38.

Kawamura, E., Himmelspach, R., Rashbrooke, M. C., Whittington, A. T., Gale, K. R., Collings, D. A. and Wasteneys, G. O. (2006). MICROTUBULE ORGANIZATION 1 regulates structure and function of microtubule arrays during mitosis and cytokinesis in the Arabidopsis root. *Plant Physiol.* **140**, 102-114.

Kirik, V., Herrmann, U., Parupalli, C., Sedbrook, J. C., Ehrhardt, D. W. and Hulskamp, M. (2007). CLASP localizes in two discrete patterns on cortical microtubules and is required for cell morphogenesis and cell division in Arabidopsis. *J. Cell Sci.* **120**, 4416-4425.

Kumagai-Sano, F., Hayashi, T., Sano, T. and Hasezawa, S. (2006). Cell cycle synchronization of tobacco BY-2 cells. *Nat. Protoc.* **1**, 2621-2627.

Liu, B. and Palevitz, B. A. (1992). Organization of cortical microfilaments in dividing root cells. *Cell Motil. Cytoskeleton* **23**, 252-264.

Lloyd, C. W. and Buschmann, H. (2007). Plant division: remembering where to build the wall. *Curr. Biol.* **17**, R1053-R1055.

Marcus, A. I., Dixit, R. and Cyr, R. J. (2005). Narrowing of the preprophase microtubule band is not required for cell division plane determination in cultured plant cells. *Protoplasma* **226**, 169-174.

McClinton, R. S. and Sung, Z. R. (1997). Organization of cortical microtubules at the plasma membrane in Arabidopsis. *Planta* **201**, 252-260.

Meng, L., Zhu, Q. and Tsai, R. Y. (2007). Nucleolar trafficking of nucleostemin family proteins: common versus protein-specific mechanisms. *Mol. Cell. Biol.* **27**, 8670-8682.

Mineyuki, Y. (1999). The preprophase band of microtubules: its function as a cytokinetic apparatus in higher plants. *Int. Rev. Cytol.* **187**, 1-49.

Mineyuki, Y., Murata, T. and Wada, M. (1991). Experimental obliteration of the preprophase band alters the sites of cell division, cell plate orientation and phragmoplast expansion in *Adiantum* protonemata. *J. Cell Sci.* **100**, 551-557.

Muller, S., Han, S. and Smith, L. G. (2006). Two kinesins are involved in the spatial control of cytokinesis in *Arabidopsis thaliana*. *Curr. Biol.* **16**, 888-894.

Muller, S., Wright, A. J. and Smith, L. G. (2009). Division plane control in plants: new players in the band. *Trends Cell. Biol.* **19**, 180-188.

Murashige, T. and Skoog, F. (1962). A revised medium for rapid growth and bioassays with tobacco tissue cultures. *Physiol. Plant.* **15**, 473-497.

Nagata, T. and Kumagai, F. (1999). Plant cell biology through the window of the highly synchronized tobacco BY-2 cell line. *Methods Cell Sci* **21**, 123-127.

Palevitz, B. A. (1987). Actin in the preprophase band of Allium cepa. *J. Cell Biol.* **104**, 1515-1519.

Paredez, A. R., Somerville, C. R. and Ehrhardt, D. W. (2006). Visualization of cellulose synthase demonstrates functional association with microtubules. *Science* **312**, 1491-1495.

Planchais, S., Glab, N., Trehin, C., Perennes, C., Bureau, J. M., Meijer, L. and Bergounioux, C. (1997). Roscovitine, a novel cyclin-dependent kinase inhibitor, characterizes restriction point and G2/M transition in tobacco BY-2 cell suspension. *Plant J.* **12**, 191-202.

Rappaport, R. (1986). Establishment of the mechanism of cytokinesis in animal cells. *Int. Rev. Cytol.* **105**, 245-281.

Sambrook, J. and Russell, D. W. (2001). Molecular cloning: a laboratory manual. Cold Spring Harbor, NY: Cold Spring Harbor Laboratory Press.

Sano, T., Higaki, T., Oda, Y., Hayashi, T. and Hasezawa, S. (2005). Appearance of actin microfilament 'twin peaks' in mitosis and their function in cell plate formation, as visualized in tobacco BY-2 cells expressing GFP-fimbrin. *Plant J.* **44**, 595-605.

Smith, L. G., Gerttula, S. M., Han, S. and Levy, J. (2001). Tangled1: a microtubule binding protein required for the spatial control of cytokinesis in maize. *J. Cell Biol.* **152**, 231-236.

Sugimoto, K., Williamson, R. E. and Wasteneys, G. O. (2000). New techniques enable comparative analysis of microtubule orientation, wall texture, and growth rate in intact roots of Arabidopsis. *Plant Physiol.* **124**, 1493-1506.

Sugiyama, N., Nakagami, H., Mochida, K., Daudi, A., Tomita, M., Shirasu, K. and Ishihama, Y. (2008). Large-scale phosphorylation mapping reveals the extent of tyrosine phosphorylation in Arabidopsis. *Mol. Syst. Biol.* **4**, 193.

Torres-Ruiz, R. A. and Jurgens, G. (1994). Mutations in the FASS gene uncouple pattern formation and morphogenesis in Arabidopsis development. *Development* **120**, 2967-2978.

Van Damme, D., Bouget, F. Y., Van Poucke, K., Inze, D. and Geelen, D. (2004). Molecular dissection of plant cytokinesis and phragmoplast structure: a survey of GFP-tagged proteins. *Plant J.* **40**, 386-398.

Van Damme, D., Vanstraelen, M. and Geelen, D. (2007). Cortical division zone establishment in plant cells. *Trends Plant Sci.* **12**, 458-464.

van Eenennaam, H., van der Heijden, A., Janssen, R. J., van Venrooij, W. J. and Pruijn, G. J. (2001). Basic domains target protein subunits of the RNase MRP complex to the nucleolus independently of complex association. *Mol. Biol. Cell* **12**, 3680-3689.

Vanstraelen, M., Van Damme, D., De Rycke, R., Mylle, E., Inze, D. and Geelen, D. (2006). Cell cycle-dependent targeting of a kinesin at the plasma membrane demarcates the division site in plant cells. *Curr. Biol.* **16**, 308-314.

Walker, K. L., Muller, S., Moss, D., Ehrhardt, D. W. and Smith, L. G. (2007). *Arabidopsis* TANGLED identifies the division plane throughout mitosis and cytokinesis. *Curr. Biol.* **17**, 1827-1836.

Wright, A. J., Gallagher, K. and Smith, L. G. (2009). discordia1 and alternative discordia1 function redundantly at the cortical division site to promote preprophase band formation and orient division planes in maize. *Plant Cell* **21**, 234-247.

Xu, X. M., Zhao, Q., Rodrigo-Peiris, T., Brkljacic, J., He, C. S., Muller, S. and Meier, I. (2008). RanGAP1 is a continuous marker of the Arabidopsis cell division plane. *Proc. Natl. Acad. Sci. USA* **105**, 18637-18642.

Journal of Cell Science